Investigation of the effect of acceleration on Taylor vortex flow using MCCDPIV

Julio Soria*, K. D. von Ellenrieder†, T. T. Lim‡ and Y. T. Chew‡

* Laboratory for Turbulence Research in Aerospace & Combustion, DME, Monash University, Clayton Campus, Melbourne, VIC 3800, Australia
e-mail: julio.soria@eng.monash.edu.au - Web page: http://LTRAC.eng.monash.edu.au

† Department of Ocean Engineering, Florida Atlantic University, SeaTech Campus, 101 North Beach Road, Dania Beach, FL 33004, USA

‡ Department of Mechanical Engineering, National University of Singapore, Singapore 119260, Singapore

ABSTRACT

The flow between two rotating concentric cylinders, known as Taylor-Couette flow, has long been the subject of theoretical and experimental investigation. As the rotational speed of the inner cylinder is slowly increased from rest, the laminar axisymmetric flow, also known as Couette flow, becomes unstable. Coles (1965) was the first to show that the final state of the flow is strongly dependent on the initial conditions and the acceleration of the inner cylinder. For a given Reynolds number, as many as 20–25 different states can be identified. As the speed changes, these states replace each other in a repeatable, but irreversible, pattern of transitions. When the inner cylinder is accelerated from rest a series of flow transitions with the following modes occurs: circular Couette flow (CCF) → Taylor vortex flow (TVF) → wavy vortex flow (WVF) → modulated wavy vortex flow (MWVF) → and turbulent Taylor vortex flow (TTVF). Lim, Chew & Xiao (1998) have shown that when the ratio η of the inner cylinder radius R_1 to the outer cylinder radius R_2 is 0.803 and the rate of change of Reynolds number is less than 2.2 secs^{-1}, the standard transition sequence of CCF → TVF → WVF exists. However, when the acceleration of the flow is higher, the final state of the flow resembles a regular Taylor vortex flow, but has a shorter axial wavelength. Further work ([7]) has shown that this "second Taylor vortex flow" (STVF) is sensitive to the geometrical properties of the flow: the Reynolds number regime over which the STVF occurs increases as the aspect ratio ($\Gamma = H/d$, where H is the height of the fluid column and $d = [R_2 - R_1]$ is the gap width) decreases and does not exist for some radius ratios outside of $\eta = 0.803$.

Generally, most experimental work on Taylor-Couette flow has been directed at understanding the stability of the flow and there are relatively few measurements of the velocity field (Wereley & Lueptow 1998). Further, most experiments have used either single point measurements, or measurements of only a single velocity component. This paper reports quantitative instantaneous in-plane velocity and out-of-plane vorticity measurements obtained using 2-component 2-dimensional (2C-2D) multigrid cross-correlation digital PIV (MCCDPIV). The instantaneous velocity fields are obtained in a plane normal to the surface of the inner cylinder when $\eta = 0.803$ and $\Gamma = 50.54$ for:

$$\frac{dRe}{dt} = 10.0\ \text{secs}^{-1}, \quad \frac{Re}{Re_{cr}} = \{1.4, 1.9, 3.5, 4.0\}, \quad \text{and} \quad \frac{dRe}{dt} = \{0.05, 0.1, 1.0, 10.0, 100.0\}\ \text{secs}^{-1}, \quad \frac{Re}{Re_{cr}} = 2.5,$$

where Re_{cr} is the critical Reynolds number denoting the onset of TVF (see figure 1).

The experiments were performed with the TC flow apparatus at the National University of Singapore. The device consists of a stationary outer perspex cyclinder, which has an inner radius of $R_2 = 94.0$ mm,

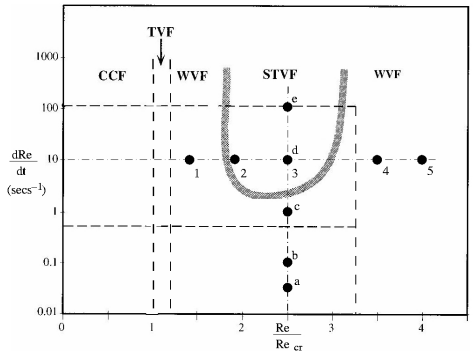

Figure 1: Transition map for Second Taylor-Couette flows. The shaded curve represents the approximate transition between WVF and STVF. PIV measurements have been made at the points indicated with a •; the numbers and lowercase letters correspond to the velocity and vorticity fields shown in figures 3, 2.

and a rotating inner aluminium cylinder of radius $R_1 = 75.5$ mm. The two cylinders are concentrically aligned along their centre axes and enclosed in a rectangular perspex tank. A computer-controlled stepper motor is used to linearly accelerate the inner cylinder from rest to a predetermined speed. The spin-up time is adjusted to achieve the desired acceleration. After the cylinder has reached the final speed, the speed is maintained for half an hour and then the PIV measurements are made. To avoid any possible "memory effects", the time interval between experiments is kept more than one hour apart. The flow is imaged by filling the gap between the cylinders with water that has been seeded with 11μm glass particles. A 5W, continuous Argon ion laser provides the illumination to create a light sheet and PIV image pairs are acquired with a CCD camera. The frame rate of the camera, and hence the time delay between each image, was fixed to 12.5 Hz.

Owing to the curvature of the cylindrical surfaces, internal reflections and optical distortion are present in the raw PIV images. These effects will generally prevent an accurate quantitative analysis of the data. A glycerol/water/sodium-iodide mixture can be matched to the refractive index of the perspex surfaces and used as a working fluid (Wereley & Lueptow 1998). This will limit the adverse geometrical effects of the TC flow apparatus, but the fluid mixture can be difficult to produce and use. Here, an alternative approach was taken. The outer rectangular tank is filled with water (no seed particles) to reduce the optical distortion created by the curvature of the outer cylinder. The raw images still contain spurious reflections on the surfaces of the inner and outer cylinders. These reflections are effectively removed, before PIV processing, by subtracting the average intensity of 50 raw images from each of the raw images.

The resulting images contain almost only seed particles and are processed using MCCDPIV analysis to yield velocity vector fields. However, the curvature of the transparent outer cylinder distorts the raw PIV images along lines normal to the surfaces of the inner and outer cylinders (often called "barrel distortion" [3]) and so the velocity vector field information must be corrected. The distortion effects in the PIV velocity data are corrected during post-processing by first transforming the images to log-polar space and correlating the image pair to determine the rotation and shift between the two images ([5]), the reconstruction coefficients necessary to transform the distorted grid into an undistorted grid are determined with a non-linear least squares fit ([3]), and then the resulting transformation is directly applied to the velocity data (see figures 3–2).

Lastly, the dimensions of the flow have a high aspect ratio. This requires one to "zoom out" and capture a relatively large region, with little resolution of small scale flow features, or to "zoom in" and resolve

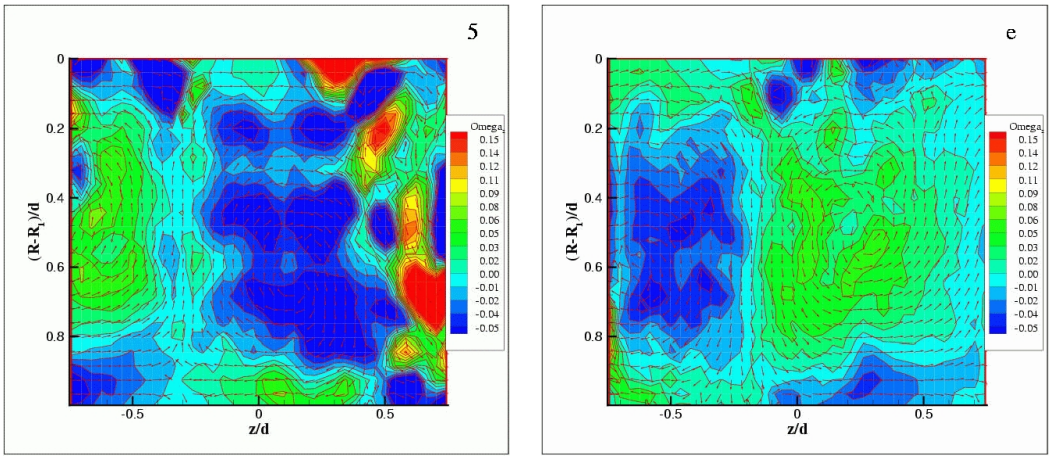

Figure 2: Velocity and vorticity (contour levels given in secs^{-1}) fields for the test points of figure 1. The z axis corresponds to the axis of symmetry of the cylinder and $z/d = 0$ is located at $H/2$.

small features but have larger scale features spill over the edges of the field of view. To circumvent the latter difficulty an autocorrelation procedure, which automatically determines the average vortex spacing in our suite of PIV images, was developed.

The leftmost columns of figures 3–2 show the velocity and vorticity fields, which result when the acceleration is fixed at $dRe/dt = 10.0\ \mathrm{secs}^{-1}$ and the Reynolds number is increased. At the low Reynolds numbers ($Re/Re_{cr} = 1.4, 1.9$) the vortices extend more than $\Delta z/d = 1.01$ in the axial direction. When $Re/Re_{cr} = 2.5$ the flow is in the STVF regime and the axial extent of the vortices decreases to about $\Delta z/d = 0.75$. At the higher Reynolds numbers ($Re/Re_{cr} = 3.5, 4$) the size of the vortices increases by about 16% and span more than $\Delta z/d = 0.88$ in the axial direction. The STVF vortices are generally smaller than WVF vortices.

The changes in the flow, which occur at a fixed Reynolds number but at various accelerations, are shown in the rightmost columns of figures 3-2. Here, as reported by Lim etal. (1998), we find that the horizontal extent of the flow decreases as the acceleration increases — the axial wavelength of the flow decreases. When the acceleration is $dRe/dt = 0.05\ \mathrm{secs}^{-1}$ the vortices are spaced more than $\Delta z/d = 0.94$ apart. For an acceleration of $dRe/dt = 100\ \mathrm{secs}^{-1}$, the spacing is about $\Delta z/d = 0.82$. However, the PIV results also reveal that the size of the structures along the radial direction increases with an increase in Reynolds number — the structures become more rectangular. The PIV results agree with the findings of Lim etal.(1998), but give extra insight into the structure of STVF.

References

[1] Coles, D. (1965) Transition in circular Couette flow. *J. Fluid Mech.* **21**, pp. 385–425.

[2] Lim, T.T. Chew, Y.T. & Xiao, Q. (1998) A new flow regime in Taylor-Couette flow. *Phys. Fluids* **10**:12, pp. 3233–3235.

[3] Raffel, M. Willert, C. & Kompenhans, J. (1998) Particle Image Velocimetry: A practical guide. Springer-Verlag.

[4] von Ellenrieder, K. D. Lim, T. T. & Soria, J. (2002) PIV measurements of second Taylor vortex flow. In *Proceedings of the 3^{rd} Australian Conference on Laser Diagnostics in Fluid Mechanics and Combustion*. Brisbane, Australia.

[5] Weiman, C. F. R. & Chaikin, G. (1979) Logarithmic spiral grids for image processing and display. *Computer Graphics and Image Processing* **11**, pp. 197–226.

[6] Wereley, S. T. & Lueptow, R. M. (1998) Spatio-temporal character of non-wavy and wavy Taylor-Couette flow *J. Fluid Mech.* **364**, pp. 59–80.

[7] Xiao, Q. Lim, T.T. & Chew, Y.T. (2002) A new flow regime in Taylor-Couette flow. *Phys. Fluids* **14**:4, pp. 1537–1539.

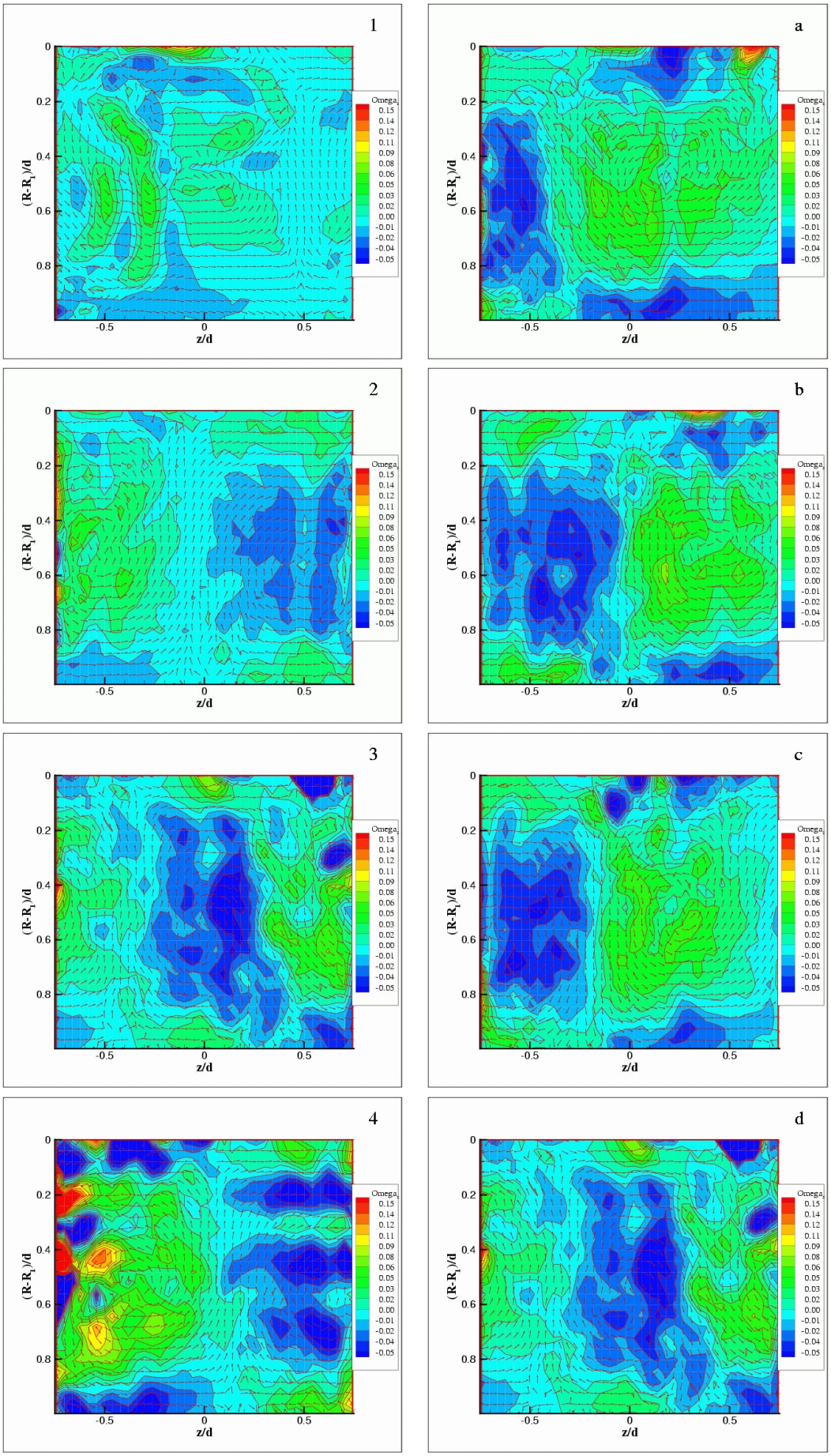

Figure 3: See caption figure 2 for description.